Project: **1163**

Project title: **C2Phase: Closure of the Cloud Phase**

Principal investigator: **Corinna Hoose, Lena Frey**

Report period: **2022-05-01 to 2023-04-30**

Statistical emulation for untangling microphysical uncertainties in hail storms

The prediction of hail storms is highly uncertain. Here, we investigate relative contributions from aerosols, microphysics and environmental conditions to the uncertainty in hail- and precipitation-related parameters. We have generated a perturbed parameter ensemble (PPE) using the ICON-ART model on convection permitting scale for one selected hail event on July 28 in 2013 over the Neckar Valley in Southwest Germany. Six parameters were jointly perturbed, namely the CCN and IN concentration, riming efficiency of graupel and hail, the stability and the vertical wind shear. We used the Latin hypercube sampling for a well-spaced distribution of the parameters in the six-dimensional parameter uncertainty space.

For the analysis of our PPE, we used two methods, statistical emulation and clustering. Statistical emulation allows us to investigate simultaneous multiple parameter perturbations in a complex numerical model at feasible computational costs. We have developed emulators for hail- and precipitation- related parameters. The emulators, informed by the so-called training runs, are used to create synthetic model output. To evaluate the predicted output from the emulator, we used additional validation runs. Using a variance-based sensitivity analysis, we were able to quantify the relative contributions from our perturbed aerosol, microphysical and environmental parameters to the uncertainty in hail- and precipitation-related variables. Figure 1 shows the contribution of the six perturbed parameters to the total precipitation. The main contributor to the total precipitation is the perturbed stability. However, we found a large diversity concerning the geographical patterns of the surface precipitation among the ensemble members from our PPE. In order to identify the controlling parameters on the geographical distribution, we used a clustering method. This approach has revealed a wind shear dependency of the geographical cluster patterns. We are still in the process of verifying the results from our clustering method with a second PPE with modified parameter ranges and will continue the analysis and development of statistical emulators.

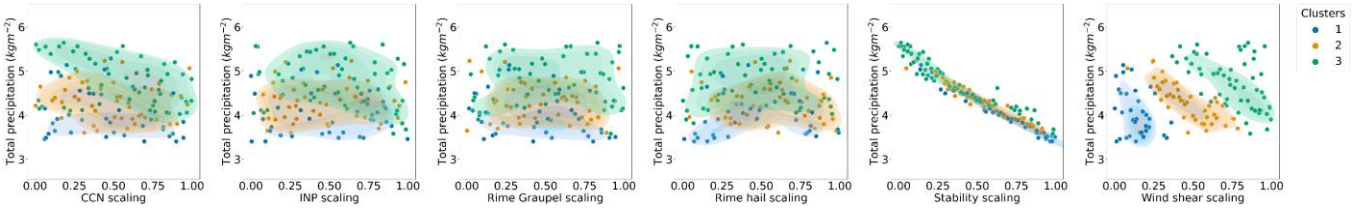

Figure 1: Domain mean of the accumulated total precipitation for all ensemble members of our PPE in dependency of the six perturbed parameters. Colours indicate 3 precipitation clusters and the contour represents a kernel density for each cluster with the lowest contour for the 0.5 iso-proportion level.

Swabian MOSES campaign in summer 2021

We have performed model simulations with the ICON-ART model on convection permitting scale for one selected day of the field campaign Swabian MOSES, where measurements were taken on the Swabian Jura during summer in 2021. We selected a day with high Saharan dust concentrations where a storm was predicted by the operational forecasts with the ICON model. Also our model simulations show the development of a storm while in reality no storm occurred. We are still in process of evaluating our model results with observations from the campaign.

Secondary ice processes

Multiple mechanisms have been proposed to explain secondary ice production (SIP), and SIP has been recognized to play a vital role in forming cloud ice crystals in some situations of convective clouds. In this study, in addition to the default rime splintering process (RS), two SIP processes, namely droplet shattering during freezing of supercooled drops (DS) and breakup

upon ice-ice collisions (BR) are implemented into a two-moment cloud microphysics scheme of ICON. Besides, two different parameterization schemes for BR are introduced. A series of sensitivity experiments is performed to investigate how SIP impacts cloud microphysics and cloud phase distributions in deep convective clouds. BR is found to dominate SIP, and the BR process rate is larger than RS and DS process rates by 4 and 3 orders of magnitude, respectively, both in ICON simulations with NWP configuration in a limited-area setup and in idealized LES experiments (see Fig.2).

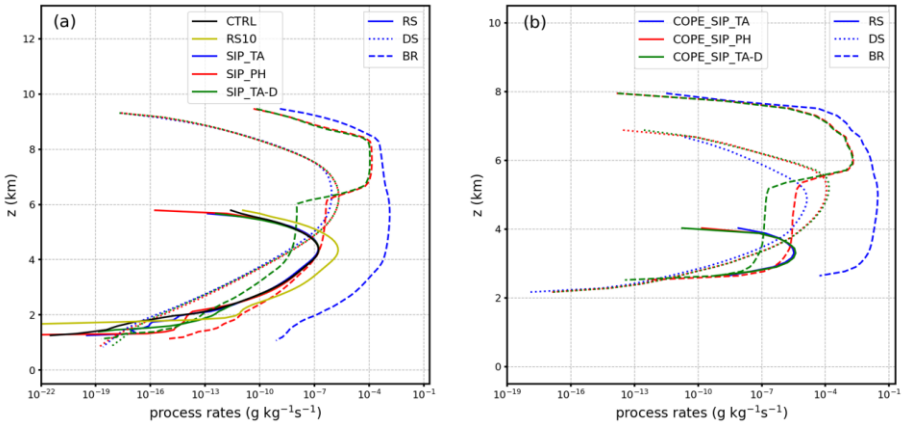

Figure 2: Spatially and time-averaged profiles over cloudy pixels of process rates for cloudy pixels of rime splintering (RS), droplet shattering (DS), and collisional breakup (BR) for (a) the NWP simulations and for (b) the idealized LES case (COPE).

Cloud types over the Arctic Ocean and Southern Ocean

Clouds with low and mid cloud base heights have been analysed in two simulations of the DYAMOND (DYnamics of the Atmospheric general circulation Modeled On Non-hydrostatic Domains) project, namely the DYAMOND Summer ICON 2.5 km run and the DYAMOND Winter ICON 2.5 km run. The analysis focuses on the region of the Southern Ocean and the Arctic Ocean, using the full simulation period except for a spin-up period of the first 10 days. A threshold of 10^{-8} kg kg^{-1} for the sum of the liquid water content and the ice water content is used to consider a grid box as cloudy. For each column, cloud base heights (CBH) and cloud top heights (CTH) are calculated and only columns with single layer clouds are considered. The atmosphere is divided into 3 layers, the lower layer from 0 km to 2 km, the middle layer from 2 km to a threshold *h* between 4 km and 7 km, which is dependent on the latitude. The clouds are then categorized by level of their cloud base height and their cloud top height, e.g., CBH and CTH of lowlevel clouds are in the range of 0 km to 2 km, while mid-lowlevel clouds have a CBH between 0 km and 2 km and a CTH between 2 km and the threshold *h* depending on the latitude. Figure 3 shows the frequency of different cloud types. We can see similar patterns for the different seasons in (a) and (b). The Southern Ocean shows a higher frequency of lowlevel clouds compared to the Arctic Ocean.

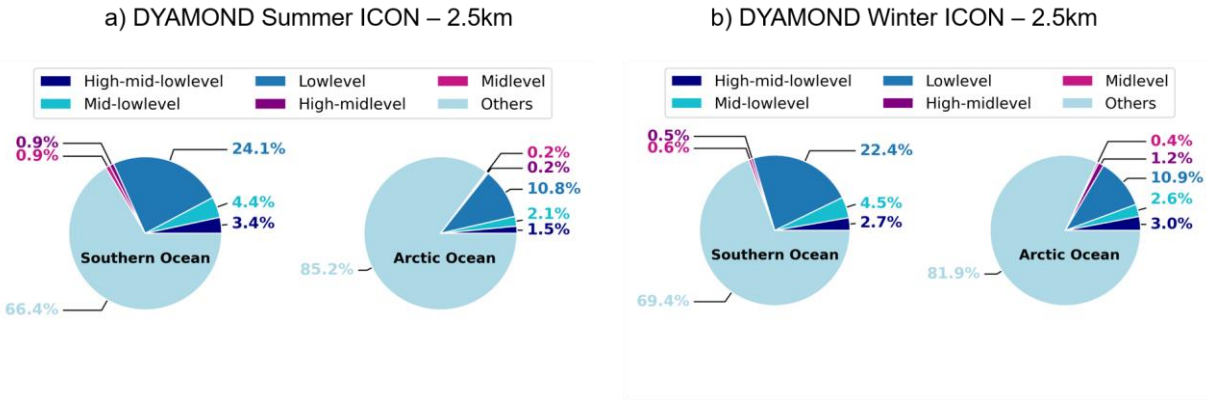

Figure 3: The pie charts show the frequency of different cloud types. Details of the methodology are described in the section above.